Variability due to short-distance favorable sound propagation and its consequences for immission assessment

T. Van Renterghem[a] and D. Botteldooren
Department of Information Technology, WAVES Research Group, Ghent University, Technologiepark 15, 9052 Gent-Zwijnaarde, Belgium

(Received 5 March 2018; revised 8 May 2018; accepted 14 May 2018; published online 7 June 2018)

The specific noise immission from an (industrial) noise source is commonly assessed by short-term measurements. Good practice prescribes measuring under downwind conditions at modest wind speeds. Nevertheless, this still leads to large variation, even at short distances and needs quantification. More specifically, the variation in sound propagation due to the changing refractive state of the atmosphere and the relatively large variation in soil impedance one can find for (visually determined) "grassland" is studied. Highly detailed meteorological tower data were combined with measured grassland impedances. These data are fed to the full-wave one-directional Green's function parabolic equation sound propagation model. The variation, even under these good-practice measurement conditions, is found to be large, and strongly dependent on sound frequency, source height, receiver height, and propagation distance. When assessing the specific sound pressure level from a multitude of sources, this variation strongly decreases compared to a low-height single source. Besides absolute variations, fluctuations in the transmission loss between a close point and a more distant one are discussed in this paper. The variation ranges give an idea on this systematic uncertainty when performing short-term measurements, and their impact on convergence to yearly averaged equivalent sound pressure levels.
https://doi.org/10.1121/1.5040483

[KVH] Pages: 3406–3417

I. INTRODUCTION

Sound pressure levels, following good practices (as, e.g., described in ISO 1996-2, Ref. 1), should be measured during (moderately) downwind episodes. This is not only to evaluate the environmental impact of the noise source when it is expected to be largest, but also to decrease variability in the measurements. The choice for downwind conditions is logical, since in case of upwind sound propagation, an acoustic shadow zone is formed at some distance from the source.[2,3] The position where this shadow zone actually starts depends—in a sensitive way—on both the source and receiver heights and the magnitude of the gradients in the sound speed profile. It is further well known—based on numerical techniques and reported experiments—that the levels in such a shadow zone (when expressed to free field sound propagation) are more or less distance independent and the degree of turbulent scattering becomes the dominant atmospheric effect.[4–6] So this sudden drop in level at some distance makes such a sound propagation condition problematic in terms of the certainty of the measured levels. Furthermore, the low levels typically experienced in such a shadow zone are likely to be dominated by other noise sources. In case of downwind sound propagation, levels are less volatile and the influence of turbulent scattering is generally less strong.[2]

However, even when performing measurements under the conditions prescribed in ISO 1996-2 (moderately downwind),[1] there will still be variation in the propagation conditions and its quantification is the goal of this work. A noise practitioner rarely has access to soil impedance data and sufficiently detailed meteorological observations (e.g., tower data); so considering the interactions between (natural) grounds and moderately downwind sound propagation conditions will quantify this variability, and can thus be used when performing short-term measurements. Manned measurement efforts during short periods (often on the order of hours) are indeed common in immission assessment of a specific noise source. Although this type of uncertainty can be categorized as *systematic* (or *epistemic*,[3] which means reducible by better information following uncertainty theory), assessing it is nevertheless relevant from a practical point of view.

This work should be seen in a bigger framework of measuring the specific immission from an (industrial) noise source in operation. This is often a difficult task. Although sound pressure level measurements (in general) have high credibility, there are nevertheless some issues. In many legislations, e.g., in the Flemish regulation regarding industrial noise,[7] an assessment of the specific noise of an installation must be made at a well-defined measurement point, i.e., either at the closest dwelling near the source, but not exceeding a distance of 200 m. At the legal assessment point, the signal-to-noise ratio might be too low to perform accurate measurements. Indeed, realistic environments typically contain many sources. Some of them are of interest, while the others are categorized as background noise. Since most industrial plants nowadays involve thorough noise planning while applying for permits, sound pressure levels are typically not excessive (which would otherwise be easy to

[a]Electronic mail: timothy.vanrenterghem@ugent.be

measure)—but this does not mean that they always adhere to the local noise regulations when in operation. Since each measurement involves uncertainties, these should be taken into account in order to draw correct conclusions in the framework of law enforcement.

In case of relatively high background noise near the assessment point, there are a few options for a sound pressure level measurement without any calculations. One can try to measure at an equivalent location at the same distance relative to the source, where the background noise is lower (e.g., further away from a nearby road than at the actual assessment spot). However, the local propagation conditions (e.g., by the presence of screening or scattering objects or soil conditions) might be different when sound travels from the source to that equivalent point. Especially in case the source has a non-uniform or unknown directivity pattern, such equivalent locations are very difficult to find.

A possible work around is first performing the measurement at closer distance to increase the signal-to-noise ratio of the source under study. In a next step, the level at the more distant legal assessment point has to be determined. One possibility is actually measuring the transmission loss between this measurement point close to the source and the legal assessment point. Such an action is, however, quite involved (and costly) since a controllable and powerful loudspeaker should be positioned near the source of interest.

A more popular approach is calculating the sound transmission between both locations in this second step. So this means that there is not only interest in the absolute variation one gets at a specific point, but also in the variation due to sound propagation between two points. A relevant question is: are there optimal locations (which means locations that are less sensitive to variations) to position the measurement points?

The main interest in this paper is the variation in sound pressure level one obtains (at a single location or as a level difference between two points) by drawing one specific case from all possible combinations of soil and refraction effects within the margins set by non-excessive downwind sound propagation over visually determined grassland. In addition, a convergence analysis is performed with this same data regarding yearly equivalent sound pressure levels by chronological sampling. This paper does not aim at studying sampling approaches like, e.g., Monte Carlo, Latin hypercube, or importance sampling that have been used to minimize measurement/computational effort to end up with converged long-term energetically averaged levels before.[3,8,9]

II. METHODOLOGY

A. Meteorological data and processing

Highly detailed meteorological data were used, available from a tower near the city of Mol, in Belgium, for the year 1997. It concerns 10-min averages of both wind speed (at 24 m, 48 m, 69 m, 78 m, and 114 m above the ground) and air temperature measured at five heights (8 m, 24 m, 48 m, 78 m, and 114 m). Wind direction was measured at three heights (24 m, 69 m, and 114 m). Relative humidity data are available from a nearby observation point on an hourly base at 1.5 m above the ground.

Sound propagation was considered around the dominant wind direction (which was south-west, 225 degrees, measured at 24 m). Favorable propagation conditions were defined as those periods falling within the wind direction range from 135 to 315 degrees. From a practical point of view, only wind was considered when defining favorable propagation conditions. Wind speed and direction are easy to measure, and an operator performing noise measurements can easily get a qualitative impression of these parameters. The vertical temperature profile is much more difficult to qualitatively estimate and quantitative data are very scarce. So this means that the selected sound speed profiles might contain upwardly refracting zones as well by not considering temperature in this (practical) definition of favorable sound propagation.

The height-dependent effective sound speed was calculated using air temperature, wind speed, and wind direction

$$c_{\mathrm{eff}}(z) = \sqrt{\kappa R T(z)} + u_{\mathrm{SR}}(z), \tag{1}$$

with κ the ratio of the specific heat capacities at constant pressure and constant volume (which is equal to 1.4 for air), R is the gas constant of dry air [287 J/(kg K)] and $T(z)$ is the height-dependent air temperature. The wind speed profile along the source-receiver line is given by $u_{\mathrm{SR}}(z)$, and has a positive sign or becomes zero for cross-wind sound propagation. For a point source, cross-wind does not alter propagation relative to neglecting wind.[10]

The meteorological observations are available at a limited number of heights, while wave-based numerical models need sound speed profiles at a high vertical resolution and at low heights as well (so below the lowest positioned sensor). Therefore, a linear-logarithmical (effective) sound speed curve will be fitted on the measured data

$$c_{\mathrm{eff}} = a_0 + a_{\mathrm{lin}} z + a_{\log} \log\left(\frac{z + z_0}{z_0}\right). \tag{2}$$

The parameters a_{lin} and $a_{\log}$ can be related to the physical parameters of theoretical-empirical flux-profile relationships for the case of a flat, homogeneous terrain.[11] This type of profile was found to provide good fits on meteorological tower data.[12] A few examples of fits on the current data set are provided in Appendix A. A value of $z_0 = 0.2$ m was found to be appropriate for the surroundings of the meteorological tower.

In this way, for each 10-min averaged meteorological observation, a unique set of values of a_0, a_{lin}, and $a_{\log}$ was available. As can be seen in Fig. 1 (yearly data), this leads to an enormous amount of cases to be calculated. Consequently, some classification was needed.

The absolute value of the effective sound speed profile is not important when modeling refraction of sound. The sound speed profiles were thus determined by the parameters a_{lin} and $a_{\log}$ only, while a_0 was fixed at 340 m/s. It is assumed that pairs with similar values would result in similar propagation conditions. In total, 146 (downwind) categories were defined, uniformly distributed over the a_{lin}–$a_{\log}$ space for this specific year, spaced at 0.25 m/s and 0.025 1/s for $a_{\log}$ and a_{lin}, respectively (see Fig. 1). The corresponding effective sound speed profiles based on these category centres are drawn in Fig. 2.

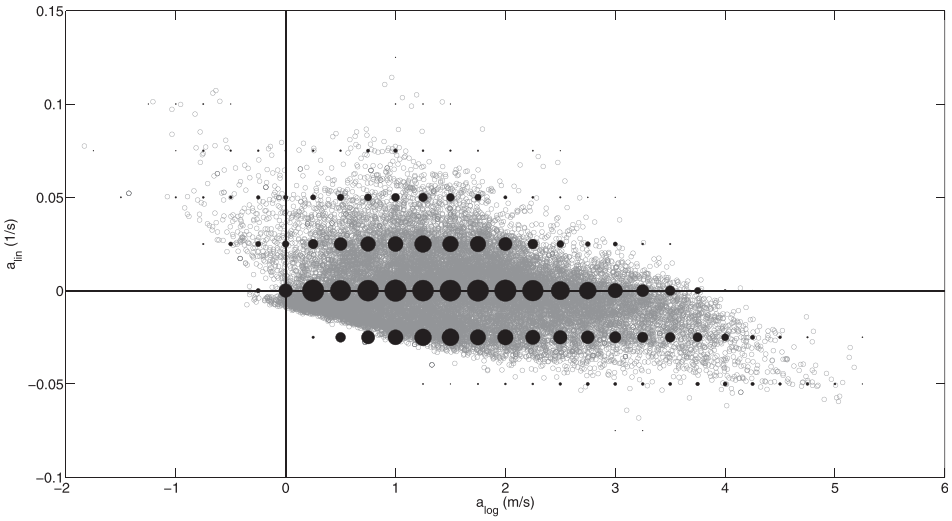

FIG. 1. Scatter plot of best-fitted $a_{\log}$-a_{lin} pairs. Only 10-min periods with moderate (see text) downwind sound propagation, relative to the most prominent wind direction, were selected. The grey circles indicate all fits, the filled black circles the categorized $a_{\log}$-a_{lin} combinations (in total 146, with their radii proportional to the number of occurrences in each class).

Relative humidity and the lowest air temperature sensor (at 8 m) were used to calculate the frequency-dependent atmospheric absorption following ISO 9613-1.[13] The influence of atmospheric pressure was neglected since its effect is insignificant.

Only 10-min averaged data with complete observations were used (which is 77.51% of the total number of records in the meteorological dataset). Of this valid data, 54.60% was categorized as non-upwind, with the additional constraint that wind speeds above 5 m/s at a (virtual) receiver height of 4 m are not considered as this would give rise to wind-induced microphone noise exceeding roughly 40 dBA (when using a 10 cm spherical windshield[14]).

B. Ground impedance data

A very common type of outdoor ground is grassland. Nevertheless, the large set of measurements summarized in Ref. 15 show that there is still a large variety in the acoustical soil impedance of grounds that could be (visually) categorized as "grassland." All types of grasslands that contain multiple measurements (and further identified as "arable," "heath," "lawn," "long grass," "pasture," "sports field," and "urban"; see Table II of Ref. 15) have been considered in the current calculations. For each of the seven types mentioned, the average values of the effective flow resistivity and effective porosity were used as shown in Table I. Although other model choices could have been made, the phenomenological[15] (Zwikker and Kosten[16]) frequency-impedance model was used, showing reasonably accurate model fits[15] over a wide range of frequencies for these types of soil. Each grassland-type was combined with all valid meteorological conditions. For a single source height, this involved $146 \times 7 = 1022$ sound propagation calculations. The effect of soil humidity was not considered, although it is likely that variation due to water content was present in the reported measurements (and their parameter fits) provided in Ref. 15.

Since the main aim is an industrial application, the first 20 m between source and receiver was modeled as rigid ground (e.g., concrete terrain). The transition to grass-covered land from the rigid source zone involves an impedance discontinuity.

C. Sound propagation modelling and parameters

The axi-symmetric Green's function parabolic equation (GFPE) method[2,17,18] was used for the sound propagation calculations over flat ground. GFPE is a reasonably

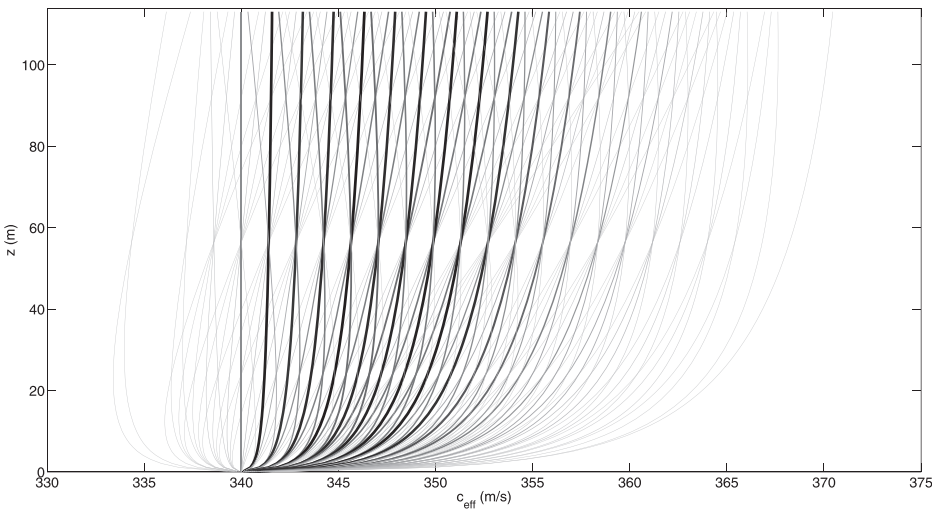

FIG. 2. Categorized effective sound speed profiles corresponding to the data presented in Fig. 1, assuming 340 m/s at ground level. The line thicknesses are proportional to the number of occurrences in each profile.

TABLE I. Effective flow resistivities and effective porosities as used in the phenomenological Zwikker and Kosten model (Ref. 16) to simulate the impedance of various types of grassland. Data based on the fits on measurements as reported in Ref. 15.

Type of grass (visual description)	Effective flow resistivity (kPa s/m^2)	Effective porosity
Arable	742	0.453
Heath	226	0.856
Lawn	216	0.763
Long grass	57	0.650
Pasture	418	0.833
Sports field	514	0.240
Urban grass	35	0.610

computationally efficient method, allowing for detailed ground effect modelling, including impedance discontinuities along the propagation path. Atmospheric refraction was simulated using the effective sound speed approach. Especially in the case of sound propagation over flat ground, vertical gradients in the horizontal component of the wind speed are the main drivers for refraction, well-captured by effective sound speed profiles. Even in more complex cases, the effective sound speed approach proves to be still quite accurate.[19,20] The refractive state of the atmosphere was assumed to be range independent. Similarly, in order not to further increase the computational cost, turbulent scattering was not considered.

GFPE needs a rather fine discretisation in the vertical direction (1/10th of the wavelength), while in the horizontal direction spatial discretisation constraints are much more relaxed. Basically, forward stepping was performed at five times the wavelength, however, with a maximum of 5 m to allow sufficient spatial resolution when presenting results. An eighth-order starter function, as described in Ref. 2, was used to initiate the calculations. An absorbing layer consisting of 500 wavelengths, exceeding the minimum advised thickness of 200 wavelengths,[21] was applied.

The 1/3 octave bands from 50 Hz to 4 kHz were considered, and ten frequencies points were explicitly calculated to constitute each band. Given the main interest in assessing the variation due to refraction and soil between a measurement and assessment point, the distances of interest are rather limited, and calculations were performed up to 250 m from the source.

Calculations were performed for two source heights, namely, 2 m and 20 m. Additional calculations were performed for two other source heights (5 m and 10 m, with equal source power and spectrum), as a proxy for a complex multi-source industrial environment. These additional source heights will not be discussed in detail in this work. Scattering or shielding by objects one could find near an industrial noise source are not considered. Since both the measurement and assessment point are thought to form a single line with the source, non-uniform source directivity, if present, should still be captured.

III. RESULTS AND DISCUSSION

The calculation results are presented as complete field plots or as a function of distance at a fixed receiver height. Common microphone heights like 1.5 m and 4 m are of main interest. More condensed analysis of variance is performed for A-weighted pink noise as source spectrum.

Given that the (temporal) distribution of levels at a single downwind location was found to be far from normally distributed, a distribution independent variation descriptor was used to present results. The 97.5th percentile ($P_{97.5}$) minus the 2.5th percentile ($P_{2.5}$) value was chosen. This range contains 95% of the observations, and is equivalent to the margins bordering four times the standard deviation in case a normal distribution would apply. Some additional graphs are shown for 68% of the distribution mass (P_{84}–P_{16}), equivalent to two times the standard deviation of a normal distribution.

A. Variation in 1/3 octave bands

When looking at individual 1/3 octave bands, the variation in sound pressure level shows a typical pattern (see Fig. 3 for a low and Fig. 4 for a high source). This variation near a low source height of 2 m and receiver height of 1.5 m is discussed here in detail. In the range of distances considered in this work, there is an approximately linear increase in variation with distance at very low frequencies. Starting from about 100 Hz, a plateau is reached, with its starting point shifting toward the source. Near 315 Hz, the magnitude of

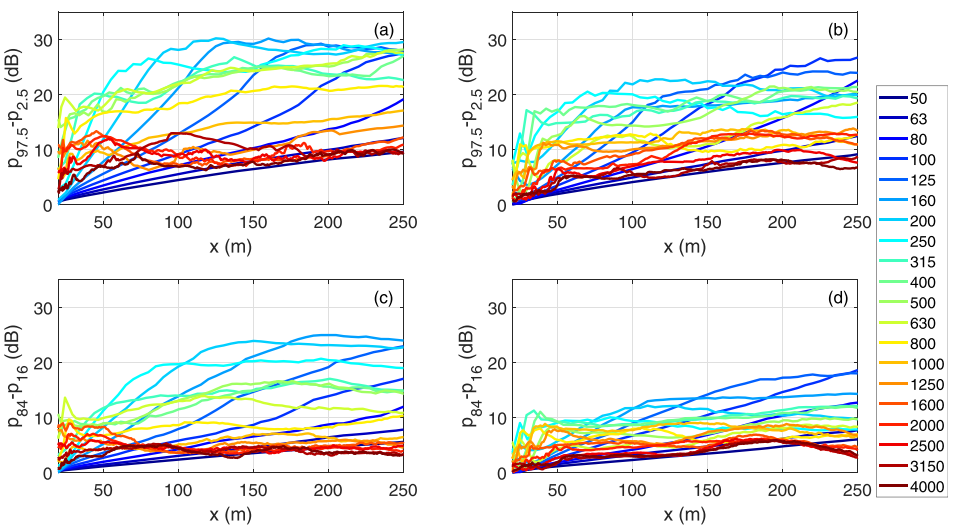

FIG. 3. (Color online) 95% ($P_{97.5}$-$P_{2.5}$) [(a) and (b)] and 68% (P_{84}-P_{16}) [(c) and (d)] variation margins in sound pressure level due to changes in moderately downwind refractive state of the atmosphere throughout the year for sound propagating over "grassland" (source height 2 m), for a receiver height at 1.5 m [(a) and (c)] and 4 m [(b) and (d)]. Each line corresponds to a different 1/3 octave band.

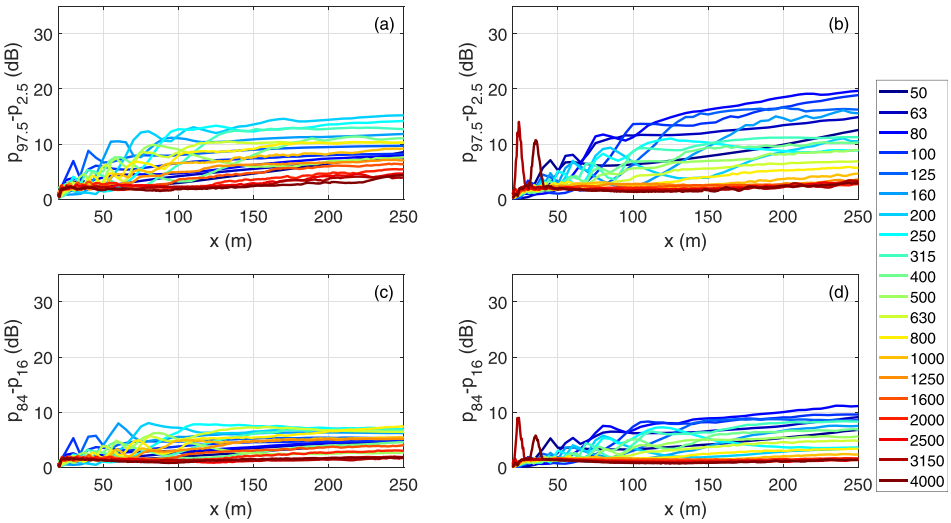

FIG. 4. (Color online) Same as in Fig. 3, but for a source height of 20 m.

this plateau starts to decrease, while above 1000 Hz a maximum in variation within 50 m from the source is observed. With increasing source and receiver height, there is a drastic decrease in the variation. At a source height of 2 m and receiver height of 1.5 m, the variation at a single 1/3 octave band can be as large as 30 dB. This variation reduces to 17 dB for a source height of 20 m and receiver at 4 m.

The strongly frequency-dependent behavior described above is consistent with observations regarding the outdoor ground effect.[22] The physical nature of this phenomenon can be explained by destructive interference, which becomes relevant in the case of natural grounds due to the additional phase shift upon interaction with the soil compared to rigid ground. Refraction of sound will lead to significant changes in path length, and multiple paths contributing to the level at a single receiver. As a result, the combination of different types of soils, and the wide range of magnitudes of the refraction effect, will lead to strong variations in the sound pressure level in the frequency range between roughly 100 Hz and 1000 Hz. This variation can be pronounced over several tens of meters. Note, however, that turbulent scattering was not considered in these simulations. This could lead to less pronounced destructive interference dips[2] in the sound pressure level and, consequently, somewhat smaller variations at such locations.

B. Variation in A-weighted pink noise: Single point source

The very strong variations in the sound pressure level one can get in individual 1/3 octave bands will be at least partly flattened out when looking at broadband noise spectra. Since broadband noise sources are of high relevance in industrial noise applications (e.g., any flow-related noise), an assessment of the variation in the sound pressure level in the case of A-weighted pink noise is made here. Note that the variation at individual bands is still of practical use, e.g., when considering tonal noise components.

1. Absolute variation

Figures 5 and 6 show field plots representing 95% of the variation in sound pressure level, by combining moderately downwind conditions over the year, and soils appearing as grassland. The overall variation in sound pressure level is strongly reduced for A-weighted pink noise compared to

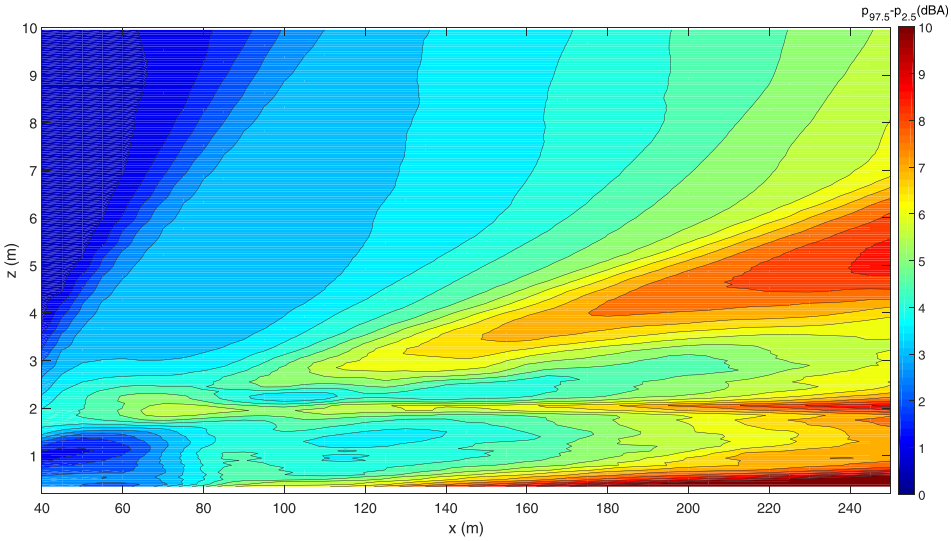

FIG. 5. (Color online) Spatial distribution of $P_{97.5}$-$P_{2.5}$ (comprising 95% of the variation) due to changes in moderately downwind refractive state of the atmosphere throughout the year for sound propagating over "grassland" (A-weighted pink noise, source height 2 m).

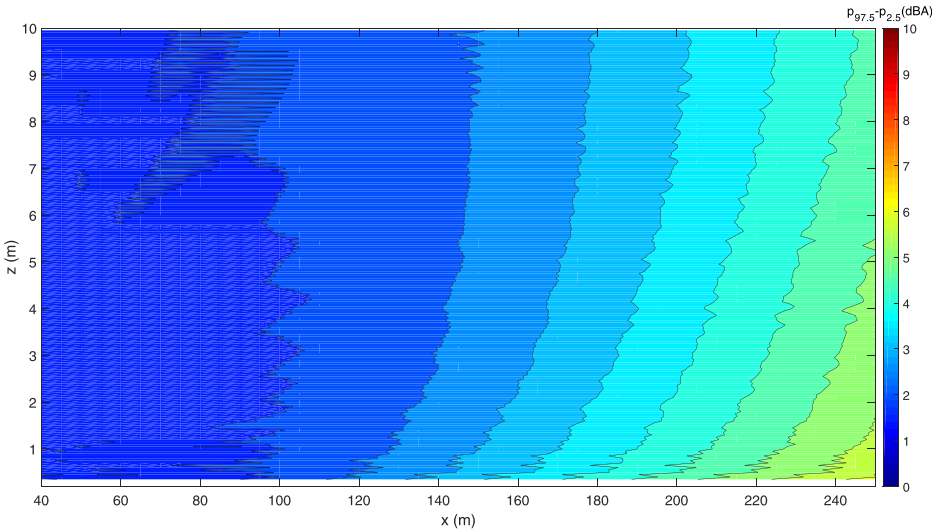

FIG. 6. (Color online) Same as in Fig. 5, but for a source height of 20 m.

individual 1/3 octave bands. This variation increases, in general, with increasing distance.

Distinct zones with higher variability are nevertheless observed at specific height ranges in the case of a low source height of 2 m. One can find such a zone very close to the ground. In addition, two other high-variability zones concentrated near the source height and near 4–5 m are observed. This finding has important practical consequences and shows that a good choice of microphone height can be relevant to minimize the uncertainty in short-term measurements. Clearly, measuring at a height of 2 m or 4 m would be less efficient here, and would need a longer period to reduce the uncertainty in the sound pressure level measurement. This variation could be roughly halved by an adequate choice of microphone location.

In the case of a much more elevated source (20 m), such strongly localized gradients in sound level variation are not found. This variation increases rather smoothly when moving closer to the ground and further away from the source. A strong overall reduction in variation compared to the low source height is found.

2. Relative variation

As discussed in the Introduction, the variation in level difference between two points along the propagation path is of practical interest. In Figs. 7–10, the 95% ranges in uncertainty were calculated for all combinations of a close measurement point x_1 and a more distant point x_2, and represented in various ways. In Figs. 7 and 9, only the part above the diagonal is of interest in practice. Typically, point x_1 is at a location with a higher signal-to-noise ratio with respect to the source under study, while the point at x_2 could be the (legal) assessment point. The variation in level difference represents the uncertainty in estimating the level at x_2 from a measurement at x_1 without accounting for instantaneous atmospheric effects and local ground conditions.

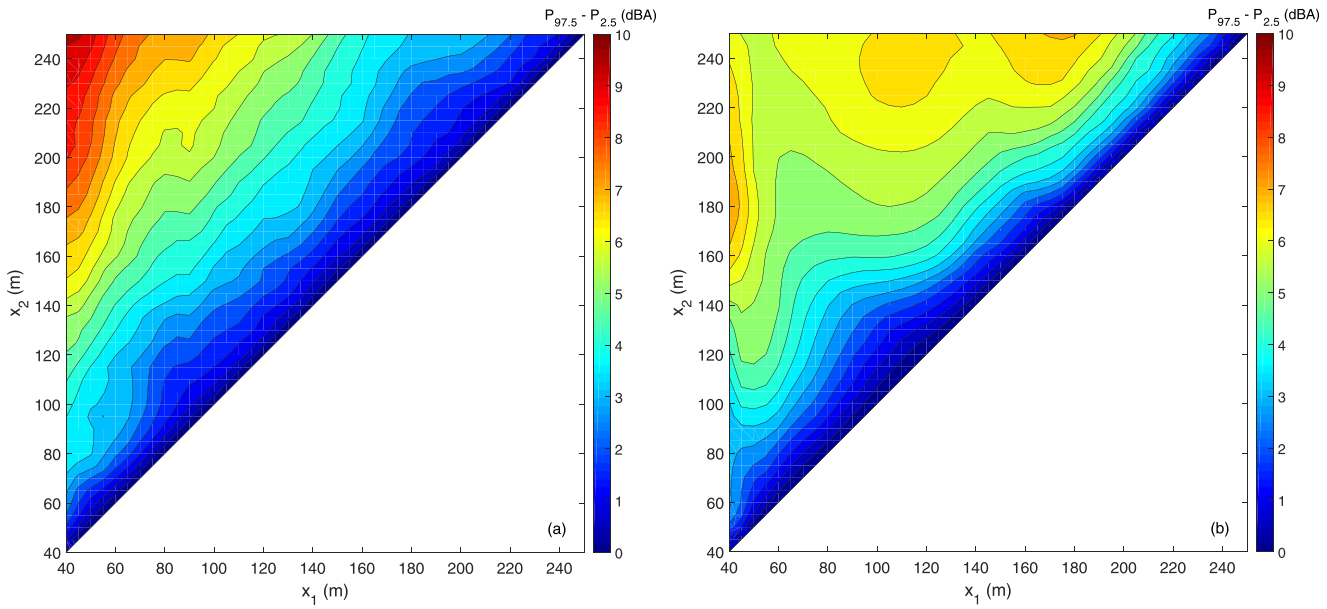

FIG. 7. (Color online) $P_{97.5}$-$P_{2.5}$ (comprising 95% of the variation) due to changes in moderately downwind refractive state of the atmosphere throughout the year for sound propagating over "grassland" of the difference in A-weighted pink noise level between two points, with $x_2 > x_1$. The source height is at 2 m; (a) receiver height 1.5 m, (b) receiver height 4.0 m (10-min averages).

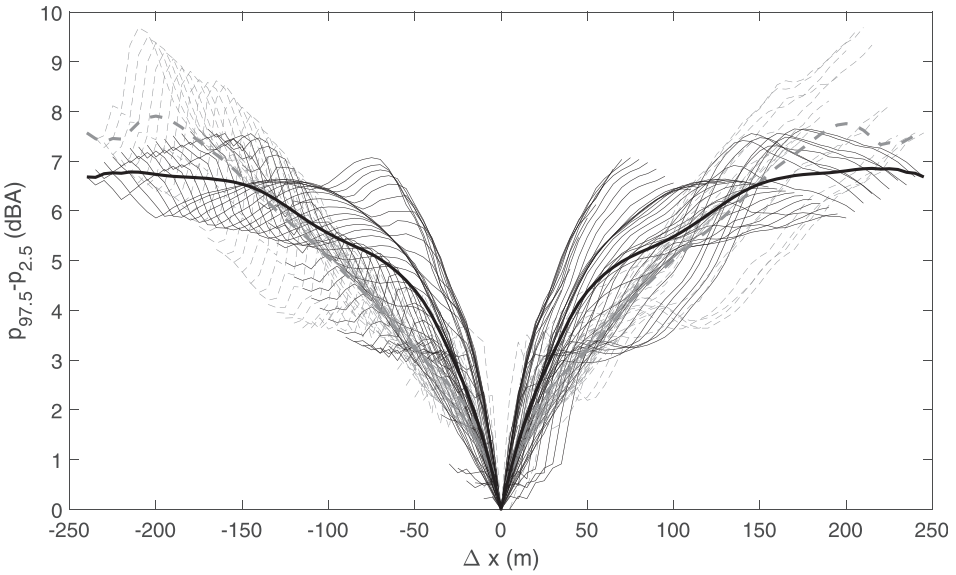

FIG. 8. Variation (due to changes in moderately downwind refractive state of the atmosphere throughout the year for sound propagating over "grassland") of the difference is A-weighted pink noise level in function of the difference in propagation distance Δx between any two points. Positive values for Δx mean that the reference point is closest to the source. The thick lines are the averages over all combinations per Δx. (Source height of 2 m, receiver height 1.5 m dashed lines, receiver height 4 m full lines, 10-min averages.)

For the low source height, when the point at x_2 is moving further away from x_1, the variation in the transmission loss increases. In case of a receiver height at 1.5 m for a point source at a height of 2 m, the 95% variation in level difference below a range difference of 50 m stays within 4 dBA (see Figs. 7 and 8). For the lower receiver height of 1.5 m, the variation in level can be large and local minima or maxima are absent. Interestingly, for the 4 m high receiver and in the case of larger separations between the two points, local minima [see Fig. 7(b)] can be found pointing at more attractive combinations. For a receiver position x_2 at 250 m from the source, position $x_1 = 60$ m is predicted to cause a lower uncertainty than moving closer to position x_2. Only starting from about $x_1 = 180$ m, the level variation drops rapidly and finally becomes zero when both points coincide.

In Figs. 8 and 10, the range difference for any combination is plotted at two fixed receiver heights. On top of these curves, the average per range difference is depicted. Also the less practical cases, namely, $x_2 < x_1$ (negative Δx) are included, which would mean positioning x_2 closer to the source than x_1. Nevertheless, this allows observing that the average curve is almost fully symmetrical. In the case of the low source height (Fig. 8), there is no clear preference for a specific receiver height. An asymptotic value is observed, with a rapid increase in variation when deviating from close separations.

For the higher source elevation of 20 m, the variation drops again strongly relative to the one predicted by the low source height at 2 m, and behaves nearly linear with separation distance. The influence of receiver height now becomes limited.

3. Convergence to long-term equivalent sound pressure levels

A relevant question is what measurement duration is needed to approach long-term equivalent sound pressure levels. For the different types of grassland, the yearly equivalent

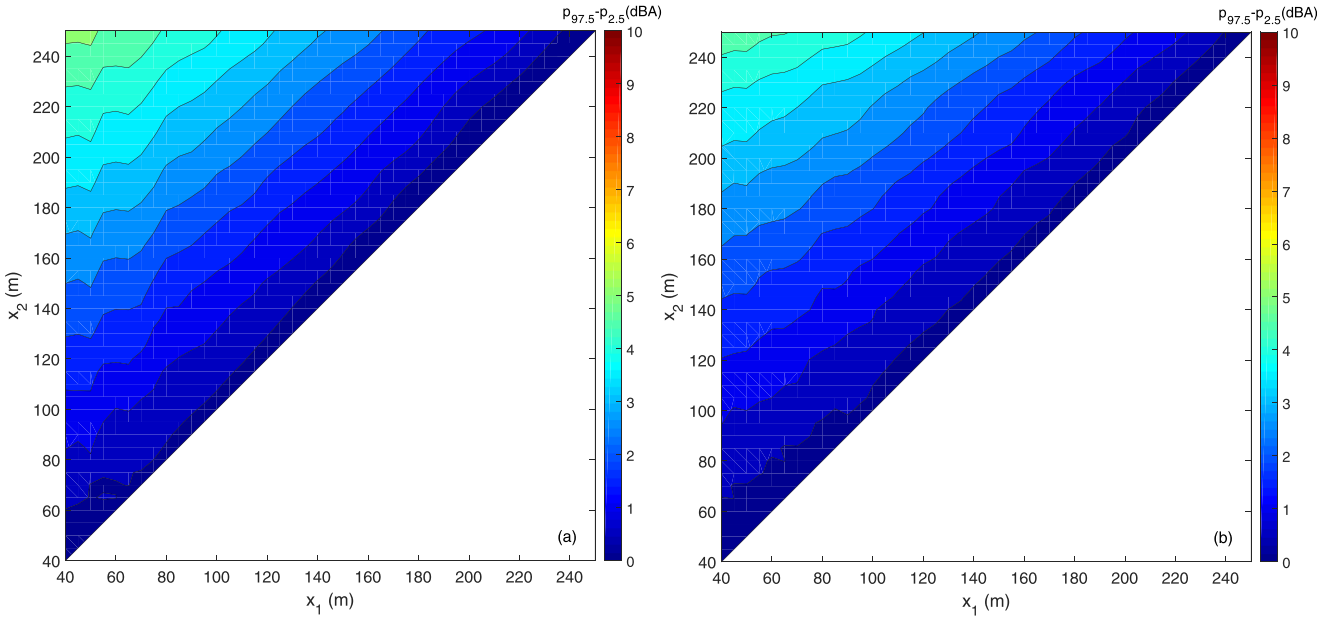

FIG. 9. (Color online) Same as in Fig. 7, but for a source height of 20 m.

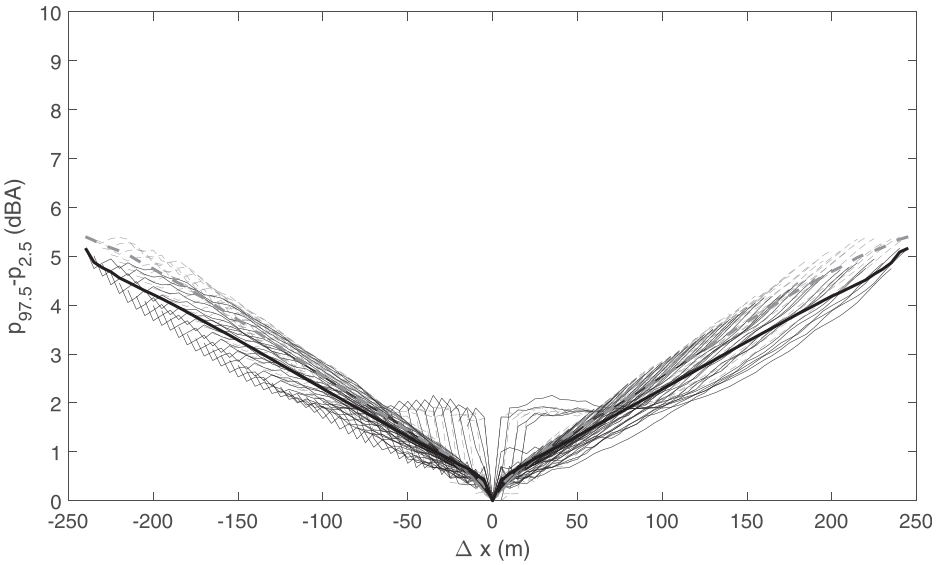

FIG. 10. Same as in Fig. 8, but for a source height of 20 m.

sound pressure level ($L_{EQ,1y}$) for (continuous) pink noise was calculated by chronologically including an increasing number of 10-min periods with moderately downwind sound propagation conditions (the nth datapoint, thus, considers all moments up to n to calculate the equivalent sound pressure level).

The starting moment of the integration will influence how the convergence to the $L_{EQ,1y}$ looks like. Fifty starting moments were defined, uniformly spread over the valid downwind episodes throughout the year under study. The first relevant (measurement) period in the specific meteorological data set (of the year 1997) was at the 14th of January at 14:40 h. For the other starting moments considered, the meteo dataset was treated cyclically to allowing capturing a full year of data as well.

Propagation distances of 50 m, 100 m, and 200 m have been defined at receiver heights 1.5 m and 4 m. This simulation was carried out separately for each of the grassland types considered in this work. The simulation results are depicted in Figs. 11 and 12, for a single source height at 2 m and 20 m, respectively. The convergence curves for the additional starting moments are indicated with the grey curves and are not intended for a detailed analysis, but show the full range of deviations one could obtain.

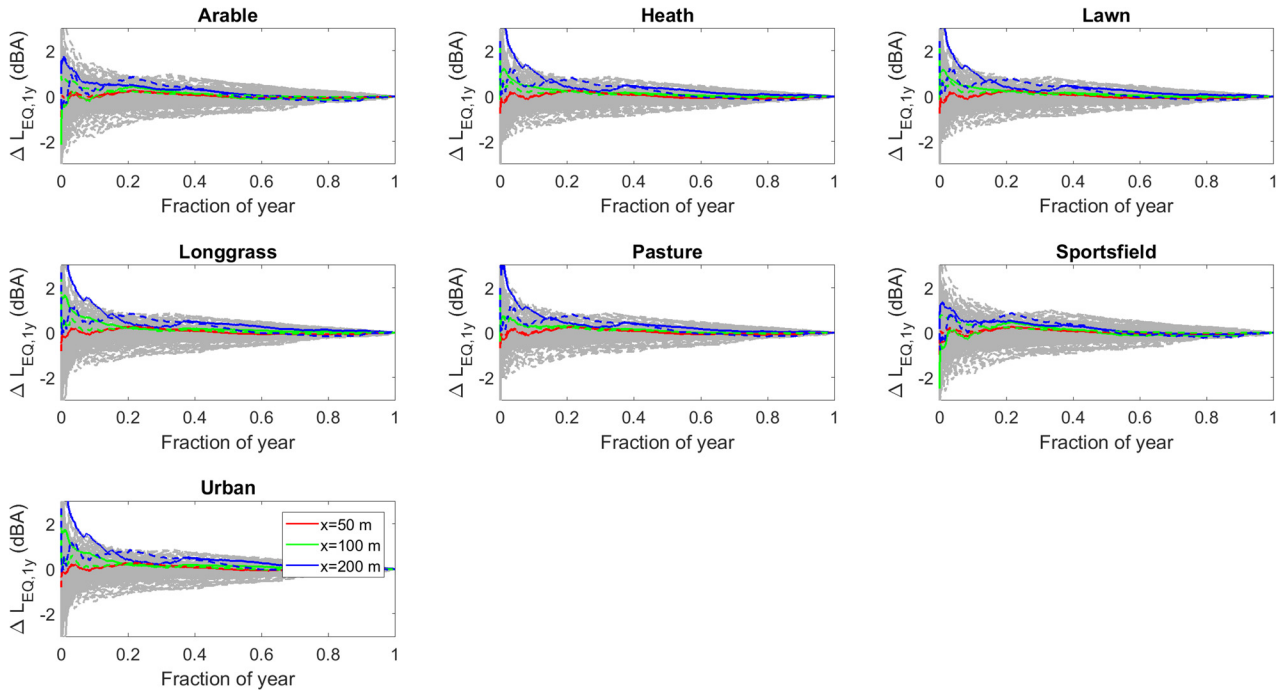

FIG. 11. (Color online) Convergence toward the yearly equivalent sound pressure levels $L_{EQ,1y}$ by chronologically adding an increasing number of (10-min averaged) downwind episodes (starting from the beginning of the year). $\Delta L_{EQ,1y}$ is the difference between the short-term (cumulatively averaged) equivalent sound pressure level and its yearly value. Three propagation distances (50 m, 100 m, and 200 m) are considered at two receiver heights (full lines 1.5 m, dashed lines 4 m) for each type of grassland separately. The additional set of (grey) background lines are for shifted starting points uniformly distributed over the year (source height of 2 m, pink noise).

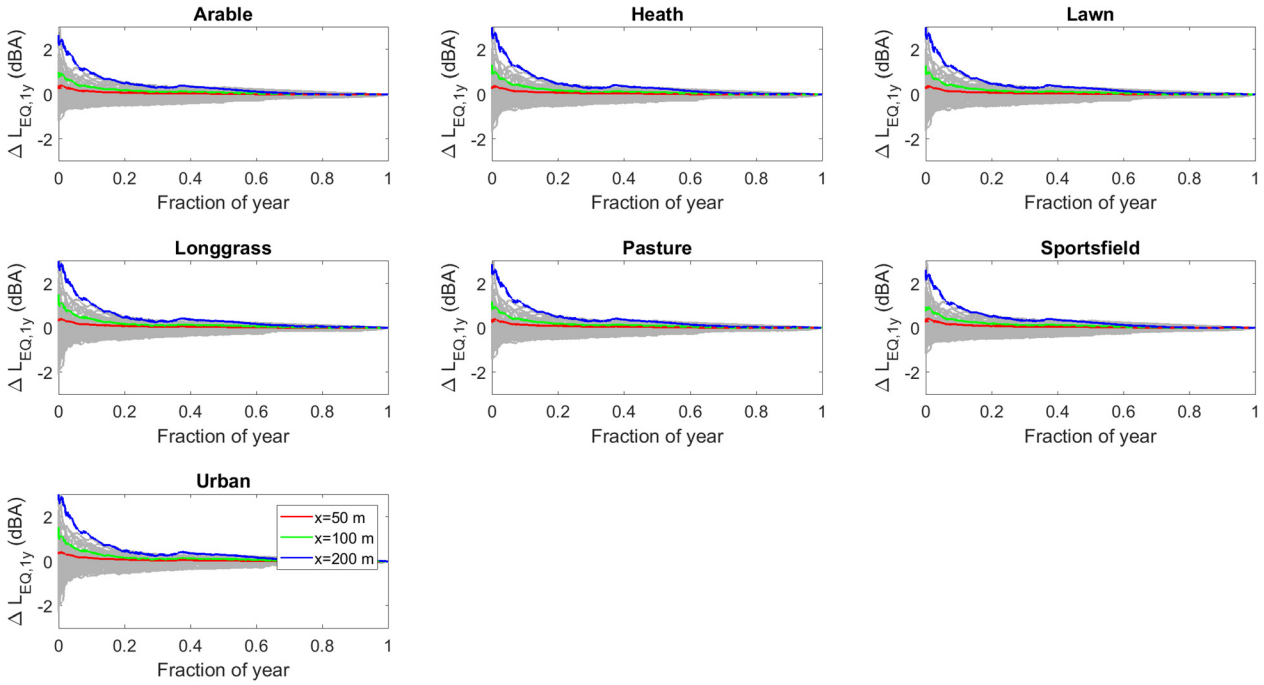

FIG. 12. (Color online) Same as in Fig. 11, but for a source height of 20 m.

With increasing propagation distance, a longer assessment period would be needed to stay within a preset maximum allowable deviation from the long-term averaged level. For a source height at 20 m, a reasonably smooth transition to the yearly averaged equivalent sound pressure level is observed at all propagation distances. To stay within 0.5 dBA, about 20% of the downwind episodes should be covered at 200 m, rather independently of the type of grassland. At 100 m, the period to be covered relaxes to roughly 5% of the year. At 50 m from the source, averaging a few downwind periods are yet sufficient. The effect of the type of grassland is rather unimportant. The choice of receiver height has a negligible effect on the simulated convergence to the long-term level. Setting the starting point at the first relevant downwind episode in the current meteorological dataset leads to an initial overestimation of the yearly equivalent sound pressure level since this specific year starts with rather strong downwardly refracting atmospheres. By considering the convergence curves for all starting moments, overall symmetry is found in this convergence, meaning that the probability for overestimation or underestimation by only considering a few episodes is similar.

For a low source height, this continuous decrease in deviation from the long-term equivalent level is not observed anymore, especially for the receiver at 200 m from the source (see Fig. 11). There is an initial strong decrease by including more periods, especially at the low receiver height of 1.5 m. The type of grassland is relevant now; grass types like arable and sportsfield seem to lead to much lower variations over time when accounting for a limited number of downwind

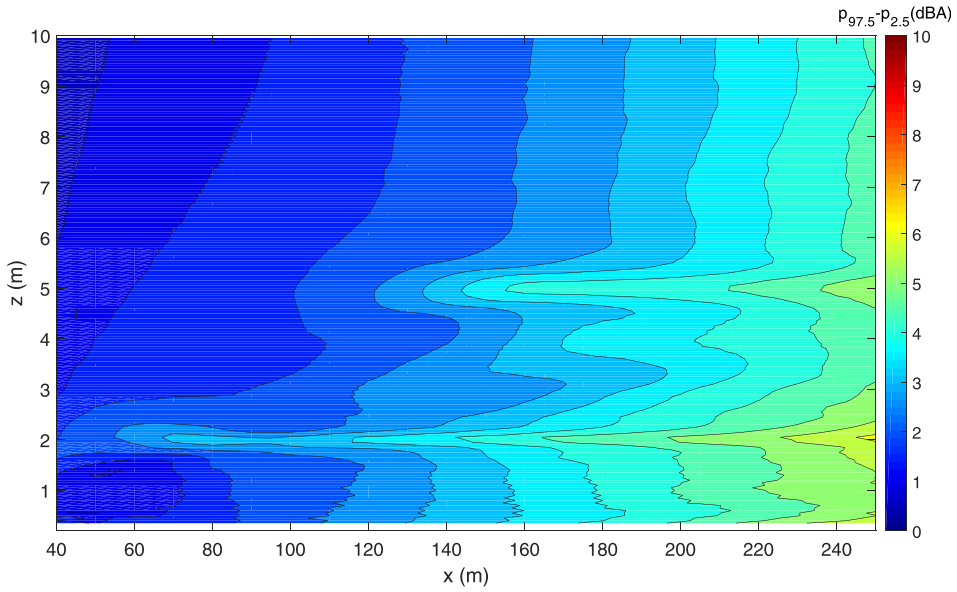

FIG. 13. (Color online) Same as in Fig. 5, but for a combination of source heights.

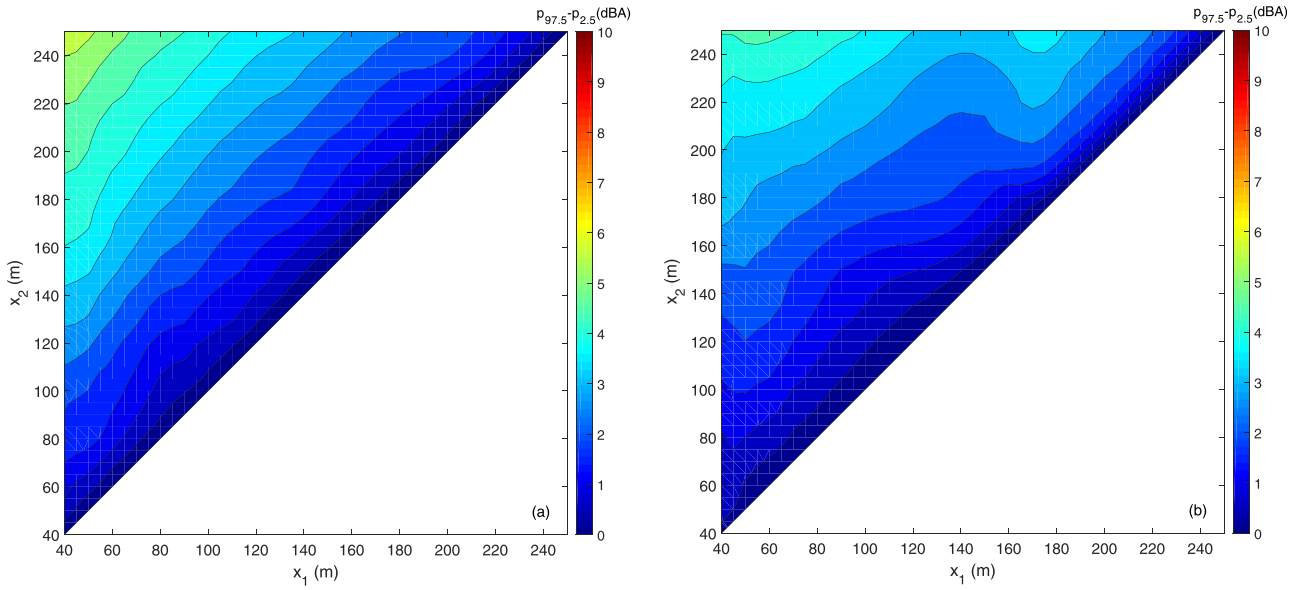

FIG. 14. (Color online) Same as in Fig. 7, but for a combination of source heights.

episodes only. A receiver height at 4 m seems a good choice when only a short measurement period is planned. This advantage relative to a receiver height at 1.5 m is less obvious when aiming at a more stringent convergence criterion of, e.g., 0.5 dBA, due to the undulating nature of the convergence curves as shown in Fig. 11. At 50 m from the source, the influence of the receiver height is very limited and a convergence criterion of 0.5 dBA is very rapidly obtained.

C. Variation in A-weighted pink noise: Multiple point sources

1. Absolute variation

A combination of source heights at 2 m, 5 m, 10 m, and 20 m was analysed to mimic a multi-source environment. These incoherent sources were positioned exactly above each other, all having equal source power and a pink noise spectrum. Absolute variations are depicted in the field plot in Fig. 13. Somewhat increased variation is still observed at the discrete source heights considered. Clearly, the overall variation is more modest than when considering a single (low) source height. A plausible physical explanation is that zones with destructive interferences resulting from one source receive (dominant) sound energy from other sources. So pronounced zones with destructive interference are less likely, and especially these are responsible for the large variations when varying soil impedances and refractive state at a single noise source.

2. Relative variation

Similarly, the relative variation between any two points is lower than in case of a (low) single source. A fully linear behavior is observed in Figs. 14 and 15, as with a single point source at higher elevation. In such a multi-source environment, a larger receiver height at 4 m now leads to a somewhat decreased variation above a separation distance of 60 m (compared to a receiver height at 1.5 m).

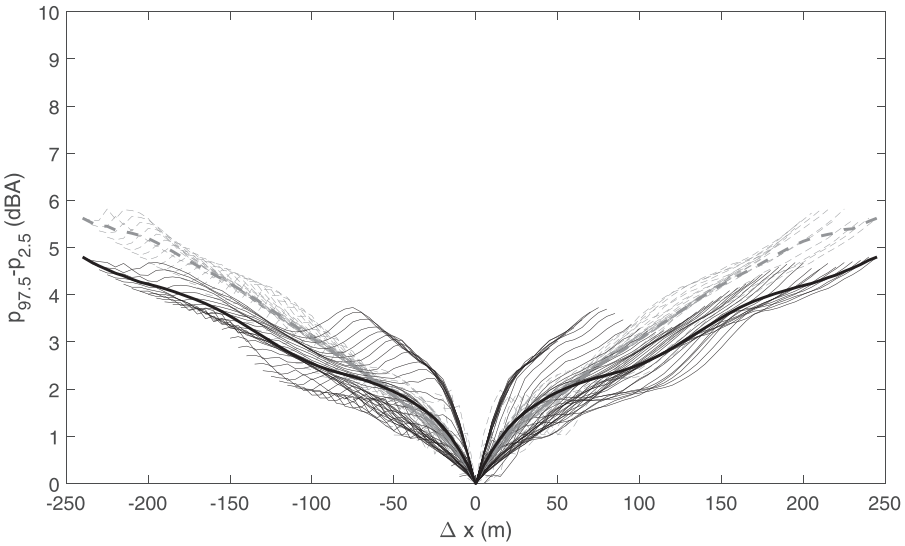

FIG. 15. Same as in Fig. 8, but for a combination of source heights.

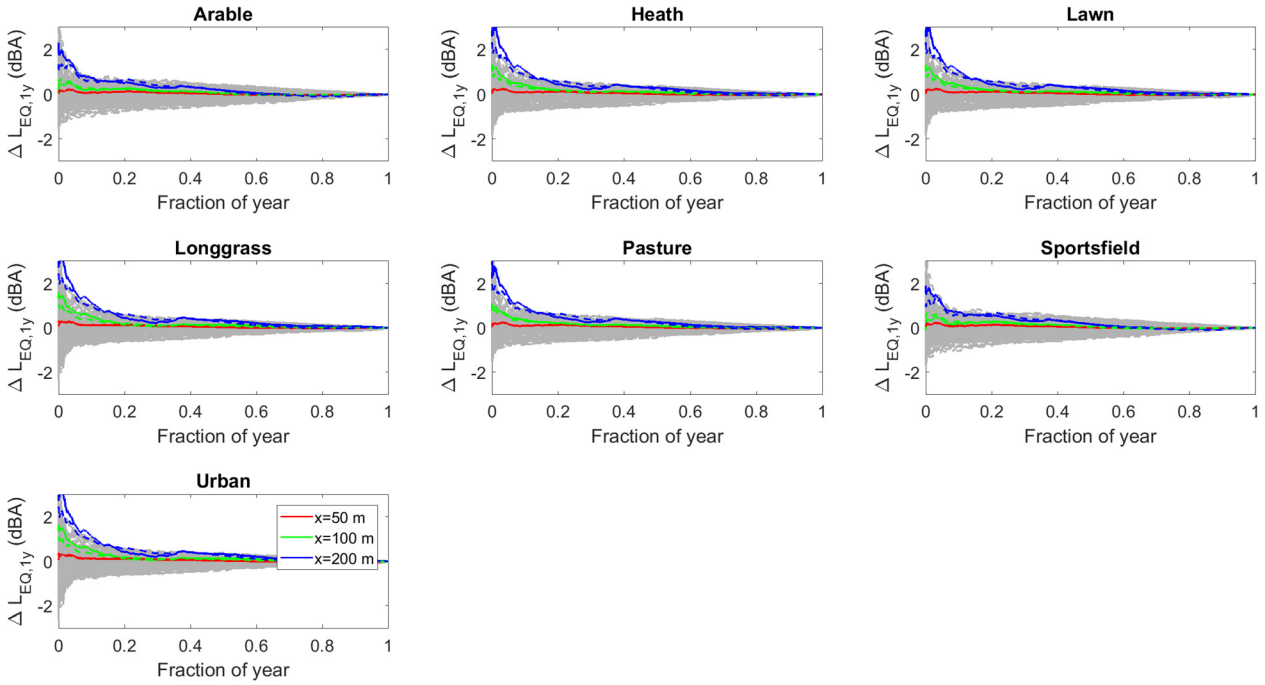

FIG. 16. (Color online) Same as in Fig. 11, but for a combination of source heights.

3. Convergence to yearly equivalent sound pressure level

A similar convergence behavior as for the elevated source height is found (see Fig. 16), indicating that due to the combination of the incoherent sound sources, ground effects become less important. There is a slight preference for a more elevated receiver height when only considering a very short measurement period.

IV. CONCLUSIONS AND LIMITATIONS

The sound pressure level variation one might observe by performing short-term measurements in moderately downwind conditions, for sound propagation over visually determined grassland, strongly depends on sound frequency (here, aggregated to 1/3 octave bands), propagation distance, source height, and receiver height. Even for relatively short propagation distances less than 250 m, this variation might be large; the 95% margins on the variation might reach 30 dB at individual 1/3 octave bands, and roughly 10 dBA in overall level for pink noise. With increasing propagation distance, this variation generally increases. In the case of more elevated sources, or when a multitude of (incoherent) sources are contributing to a single receiver, this variation generally drops compared to single or low noise sources. A good choice of receiver height might lead to a significant decrease in the variation observed by performing short-term measurements and should thus be considered to more rapidly converge to the long-term equivalent sound pressure level when assessing continuous noise sources.

Similarly, the variation in sound pressure level between any two points along the propagation path increases with separation distance. In some cases, there are preferred positioning combinations. The numerical results presented in this work can be used to estimate the sound pressure level uncertainty at a more distant point when a close-by measurement is available, and when there is no information (which is common) about the (specific) refractive state of the lower part of the atmosphere and *in situ* ground impedance.

The current paper did not consider turbulent scattering and non-flat grounds as additional sources of uncertainty in propagation. Especially ground undulations, even small ones, can have a rather strong effect on near-ground sound propagation. Not only terrain focusing (concave ground[23]) or shielding (convex ground[24]) could be relevant, but also their interactions with the ground impedance and their influence on the refractive state of the lower part of the atmosphere. This could be an additional cause of uncertainty, probably leading to a further increase in the sound pressure level variation compared to assuming flat ground. Turbulent scattering is expected to be mainly relevant for single source conditions and in individual 1/3 octave bands under the downwind propagation conditions considered in the current analysis. Given that the presence of destructive interferences drive this level variation, including turbulent scattering might actually give rise to a smaller amount of variation. However, more research is needed to confirm this statement.

General modeling inaccuracies will add to the uncertainty in transmission corrections, which was not the aim of the current work. The parabolic equation method is used, which is a full-wave (directional) sound propagation model and is considered to be reasonably accurate. Detailed (measured) ground impedance data and meteorological tower data at high temporal resolution are used in these simulations to increase realism.

APPENDIX A: EXAMPLE FITS OF LOGARITHMIC-LINEAR SOUND SPEED PROFILES ON METEOROLOGICAL TOWER DATA

A selection of fitted effective sound speed profiles, determined using Eqs. (1) and (2), are shown in Fig. 17.

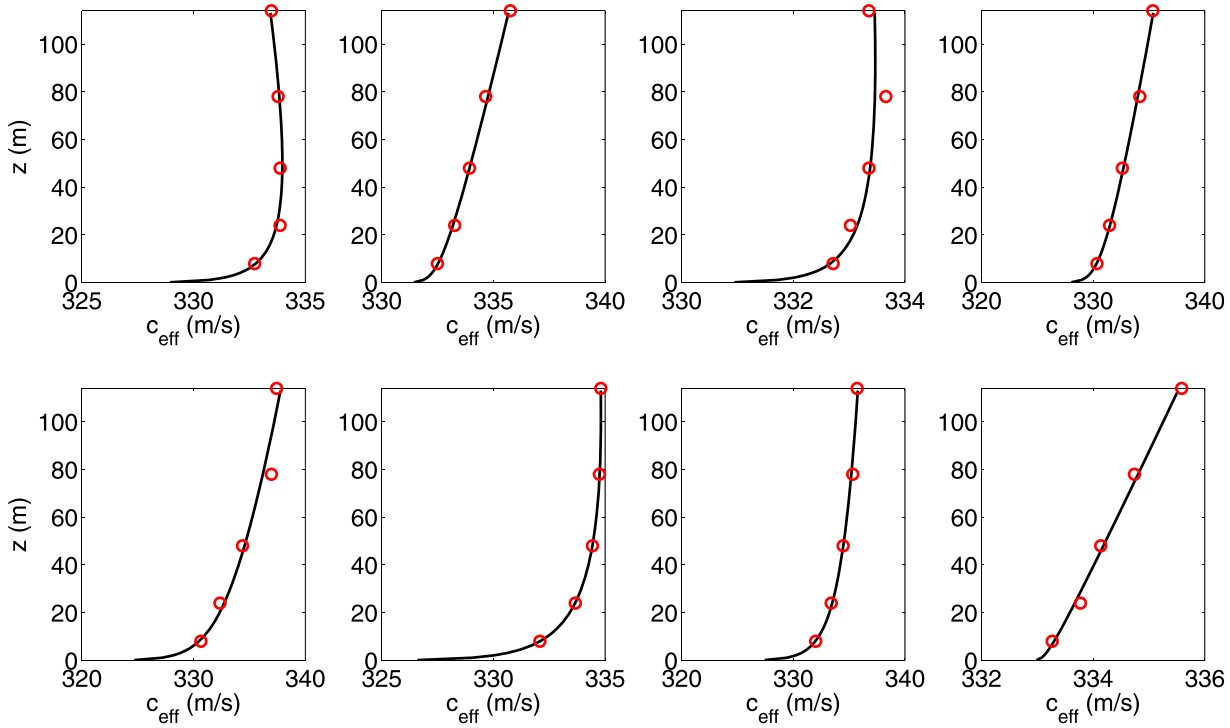

FIG. 17. (Color online) Random selection of fitted effective sound speed profiles (full lines); the open circles depict the effective sound speeds at the sensor heights (10-min averages).

Only downwind conditions, following the selection criteria as discussed in Sec. II, are considered.

[1]ISO 1996-2: *Acoustics—Description, Measurement and Assessment of Environmental Noise. Part 2: Determination of Sound Pressure Levels* (International Organisation for Standardisation, Geneva, Switzerland, 2017).

[2]E. Salomons, *Computational Atmospheric Acoustics* (Kluwer, Dordrecht, The Netherlands, 2001), 335 pp.

[3]V. Ostashev and D. K. Wilson, *Acoustics in Moving Inhomogeneous Media*, second ed. (CRC Press, Boca Raton/Taylor and Francis, London, 2016), 521 pp.

[4]K. Gilbert and R. Raspet, "Calculation of turbulence effects in an upward refracting atmosphere," J. Acoust. Soc. Am. **87**, 2428–2437 (1990).

[5]R. Raspet and W. Wu, "Calculation of average turbulence effects on sound propagation based on the fast field program formulation," J. Acoust. Soc. Am. **97**, 147–153 (1995).

[6]P. Chevret, P. Blanc-Benon, and D. Juvé, "A numerical model for sound propagation through a turbulent atmosphere near the ground," J. Acoust. Soc. Am. **100**, 3587–3599 (1996).

[7]VLAREM II: "Besluit van de Vlaamse regering van 1 juni 1995 houdende algemene en sectorale bepalingen inzake milieuhygiëne" ("General and specific Flemish regulation regarding environmental care") (in Dutch).

[8]C. Pettit and D. K. Wilson, "Proper orthogonal decomposition and cluster weighted modeling for sensitivity analysis of sound propagation in the atmospheric surface layer," J. Acoust. Soc. Am. **122**, 1374–1390 (2007).

[9]D. K. Wilson, C. Pettit, V. Ostashev, and S. Vecherin, "Description and quantification of uncertainty in outdoor sound propagation calculations," J. Acoust. Soc. Am. **136**, 1013–1028 (2014).

[10]M. Hornikx and T. Van Renterghem, "Numerical investigation of the effect of crosswind on sound propagation outdoors," Acta Acust. Acust. **102**, 558–565 (2016).

[11]D. Heimann, M. Bakermans, J. Defrance, and D. Kühner, "Vertical sound speed profiles determined from meteorological measurements near the ground," Acta Acust. Acust. **93**, 228–240 (2007).

[12]D. Heimann and E. Salomons, "Testing meteorological classifications for the prediction of long-term average sound levels," Appl. Acoust. **65**, 925–950 (2004).

[13]ISO 9613-1: *Acoustics—Attenuation of Sound during Propagation Outdoors—Part 1* (International Organisation for Standardisation, Geneva, Switzerland, 1996).

[14]G. van den Berg, "Wind-induced noise in a screened microphone," J. Acoust. Soc. Am. **119**, 824–833 (2006).

[15]K. Attenborough, I. Bashir, and S. Taherzadeh, "Outdoor ground impedance models," J. Acoust. Soc. Am. **129**, 2806–2819 (2011).

[16]C. Zwikker and C. W. Kosten, *Sound Absorbing Materials* (Elsevier, New York, 1949).

[17]K. Gilbert and X. Di, "A fast Green's function method for one-way sound propagation in the atmosphere," J. Acoust. Soc. Am. **94**, 2343–2352 (1993).

[18]E. Salomons, "Improved Green's function parabolic equation method for atmospheric sound propagation," J. Acoust. Soc. Am. **104**, 100–111 (1998).

[19]R. Blumrich and D. Heimann, "Numerical estimation of atmospheric approximation effects in outdoor sound propagation modelling," Acta Acust. Acust. **90**, 24–37 (2004).

[20]T. Van Renterghem, D. Botteldooren, and P. Lercher, "Comparison of measurements and predictions of sound propagation in a valley-slope configuration in an inhomogeneous atmosphere," J. Acoust. Soc. Am. **121**, 2522–2533 (2007).

[21]J. Cooper and D. Swanson, "Parameter selection in the Green's function parabolic equation," Appl. Acoust. **68**, 390–402 (2007).

[22]K. Attenborough, K. M. Li, and K. Horoshenkov, *Predicting Outdoor Sound* (Taylor and Francis, London, 2007), 485 pp.

[23]Q. Wang and K. M. Li, "Sound propagation over concave surfaces," J. Acoust. Soc. Am. **106**, 2358–2366 (1999).

[24]K. M. Li, Q. Wang, and K. Attenborough, "Sound propagation over convex impedance surfaces," J. Acoust. Soc. Am. **104**, 2683–2691 (1998).